Accepted Manuscript

Polar snow algae as a valuable source of lipids?

Chris J Hulatt, Orsolya Berecz, Einar Skarstad Egeland, René H Wijffels, Viswanath Kiron

PII: S0960-8524(17)30411-X
DOI: http://dx.doi.org/10.1016/j.biortech.2017.03.130
Reference: BITE 17834

To appear in: *Bioresource Technology*

Received Date: 24 January 2017
Revised Date: 17 March 2017
Accepted Date: 22 March 2017

Please cite this article as: Hulatt, C.J., Berecz, O., Egeland, E.S., Wijffels, R.H., Kiron, V., Polar snow algae as a valuable source of lipids?, *Bioresource Technology* (2017), doi: http://dx.doi.org/10.1016/j.biortech.2017.03.130

Polar snow algae as a valuable source of lipids?

Chris J Hulatt[1]*, Orsolya Berecz[1], Einar Skarstad Egeland[1], René H Wijffels[1,2], Viswanath Kiron[1]

[1]Faculty of Biosciences and Aquaculture, Nord University, Bodø, Norway.

[2]Bioprocess Engineering, AlgaePARC, Wageningen University, Wageningen, The Netherlands.

*Corresponding author:

Chris J Hulatt

chrisjhulatt@gmail.com; christopher.j.hulatt@nord.no

Tel (+47) 9009 8564

Words in Main Text: 4,054

Words in abstract: 149

Figures: 6

Tables: 5

1 Supporting file

1 Graphical Abstract

ABSTRACT

Microalgae offer excellent opportunities for producing food and fuel commodities, but in colder climates the low growth rates of many varieties may hamper production. In this work, extremophilic Arctic microalgae were tested to establish whether satisfactory growth and lipid production could be obtained at low water temperature. Five species of snow/soil algae originating from Svalbard (78-79°N) were cultivated at 6°C, reaching high cell densities (maximum dry weight 3.4 $g \cdot L^{-1}$) in batch cultivations, and high productivity (maximum 0.63 $g \cdot L^{-1} \cdot d^{-1}$). After 20 days of cultivation total lipids ranged from 28 to 39% of the dry weight, and diverse patterns of neutral lipid (triacylglycerol; TAG) accumulation were observed. The five species largely accumulated unsaturated fatty acyl chains in neutral lipids, especially polyunsaturated C16 series fatty acids, C18:1*n*-9 and C18:3*n*-3. The results indicate that polar microalgae could provide an opportunity to increase the yields of microalgal biomass and oil products at low temperatures.

KEYWORDS

Microalgae; Arctic; photobioreactor; triacylglycerol (TAG); snow algae

1. INTRODUCTION

Microalgae are single-cell factories that may find applications as biofuel, feed and food production platforms (Georgianna & Mayfield 2012; Hu et al., 2008). Cultivating these fast-growing microorganisms on marginal land using waste or saline water supplies offers promising solutions to global food, climate and energy issues, yet producing algal biomass at scale with low environmental impacts still faces several challenges (Canadell & Schulze, 2014; Chisti, 2013; Matassa et al., 2016). A major technical challenge is that production of microalgae biomass and oil in colder climates can be inefficient, because common strains such as those used for commercial work produce low yields at temperatures below ~15°C (Chisti 2012; Moody et al., 2014). However, by selecting alternative species from cold polar habitats, it may be possible to mitigate some of the effects of cold temperatures on productivity (Varshney et al., 2015).

Typical strains of microalgae used for commercial applications in outdoor raceway ponds and photobioreactors require warm waters of around 24-40°C to attain their optimal growth rates (Bernard & Rémond 2012; Béchet et al., 2011; Chisti 2012; Endres et al., 2016). At higher latitudes, this could limit efficient production of model microalgae species to summer months, or require heating of the culture broth, consuming large amounts of energy (Moody et al., 2014). However, ecological research has shown for some time that microalgae can be surprisingly productive in very cold environments (Komárek et al 2007; Leya et al., 2009; Lutz et al., 2016; Lyon & Mock 2014; Mock et al., 2017; Thomas & Dieckmann 2002), indicating that cold-adapted strains could mitigate some of the effects of low temperature on bioprocess efficiency.

Below a thermal optimum, metabolic rate invariably reduces with decreasing temperature. The effect is predictable, because metabolism is a network of enzyme-catalyzed (i.e. temperature dependent) reactions, which can generally be described by

exponential (Q_{10}) or log-linear Arrhenius functions (Ahlgren et al., 1987; Falkowski & Raven 2013; Raven & Geider 1988). Though this indicates microalgae should invariably grow slowly in cold conditions, the microbes inhabiting permanently cold regions have experienced strong, persistent selection and have acquired a range of physiological adaptations that allow them to succeed at temperatures close to, or even below freezing (Cavicchioli et al., 2011; Gounot & Russell 1999; Morgan-Kiss et al., 2006). One of these adaptations is the increased abundance of polyunsaturated fatty acids (PUFAs) in the lipids of cold-adapted microalgae, which improve the performance of biological membranes, key sites of metabolism, at lower temperatures (Morgan-Kiss et al., 2006). Cold-adapted microalgae may therefore offer lipid products enriched in PUFAs, with potential uses in biotechnology and industrial products.

Cold environments can however differ considerably in other physical and chemical variables. For example, microalgae inhabiting sea-ice are exposed to constantly low temperatures and low light conditions, often with substantial variations in salinity (Mock et al., 2017, Thomas & Dieckmann, 2002). Alternatively, terrestrial species of microalgae found on snow, ice, rock, soil crusts and glaciers, often termed snow-algae, are of special interest because they can survive under high irradiance and unstable temperature regimes (Hori et al., 2014). These conditions are analogs to those often occurring in outdoor photobioreactors and shallow raceway ponds, making this group potentially interesting for industrial applications in harsh climates.

To test whether cold-adapted microalgae could offer solutions for industrial cultivation in colder temperatures, terrestrial chlorophyte microalgae originating from the Svalbard archipelago (74 to 81°N) were selected (Table 1). These microbes experience persistently low temperatures and extreme annual variations in photoperiod (24 h dark to 24 h sunlight). Five test strains were cultivated in an array of low-

temperature photobioreactors supplied with concentrated CO_2 to study their growth, photosynthetic efficiency and neutral lipid production in batch and semi-continuous cultures. A temperature of 6°C was selected for testing, because it is substantially lower than other bioreactor studies.

2. MATERIALS & METHODS

2.1. Bioreactor cultivation

Five varieties of microalgae (Table 1) were obtained from the Culture Collection of Cryophilic Algae (CCCryo, Fraunhofer, Germany). Each strain was originally collected from snowfields and solid substrates on Spitsbergen (Svalbard, 78-79°N, 11°E). Prior to experiments the cultures were maintained in Erlenmeyer flasks at 2-4°C at an irradiance of 30 ± 10 $\mu mol \cdot m^{-2} \cdot s^{-1}$ provided by a 4700K color temperature fluorescent lamp. The experimental equipment comprised a temperature-controlled environment chamber (Termaks AS, Bergen, Norway) fitted with nine fluorescent lamps (cool daylight, 36W, Phillips) containing 12 photobioreactor units. Photobioreactors were 350 mL glass tubes (Friedel, Oslo, Norway) measuring 35 mm internal diameter. They contained 310 mL of media, fitted with sealed silicone stoppers and autoclaved as complete units. Carbon dioxide enriched gas (60 $mL \cdot min^{-1}$) was supplied to each photobioreactor by rotameter (Omega, Manchester, UK). The CO_2 concentration was controlled by mixing dried, filtered, compressed air with carbon dioxide using a mass flow control system (GMS-150, Photon Systems Instruments, Czech Republic) (Figure 1). Experimental replication was achieved by repeating each treatment 3 or more times. Each strain was initially assigned to one of the bioreactors at random, then subsequently moved amongst reactors for each replicate to mitigate any small reactor-specific effects. Photobioreactors were

illuminated from one side at an irradiance of 135 $\mu mol \cdot m^{-2} \cdot s^{-1}$ (batch cultures) or 230 $\mu mol \cdot m^{-2} \cdot s^{-1}$ (semi-continuous cultures). To measure the light conversion efficiency the average irradiance over the photobioreactor surface was calculated. This was done by measuring the photon flux normal to the glass wall (transmittance = 0.96) at twelve evenly spaced positions on each of the units (0, 90, 180, 270° to the light source at top, middle and base) at each irradiance level. For batch cultures the average irradiance measured 67.9 ± 2.1 $\mu mol \cdot m^{-2} \cdot s^{-1}$ ($M \pm SD$, $n = 12$) whilst for semi-continuous cultures this increased to 116.2 ± 5.0 $\mu mol \cdot m^{-2} \cdot s^{-1}$ ($M \pm SD$, $n = 12$). These were expressed as a daily photon flux, f_{day}, with units $mol \cdot m^{-2} \cdot d^{-1}$. Thirty batch cultures were conducted (5 strains × 2 time points × 3 replicates) with a CO_2 concentration of 1% v/v. Batch cultures used Bolds Basal Medium (BBM, Bischoff & Bold, 1963) with double-strength $NaNO_3$ (5.88 mM). Semi-continuous cultures used increased CO_2 concentrations (2.5%) and triple-strength $NaNO_3$ (8.82 mM), to ensure that nutrients were always provided in excess. Semi-continuous cultivations were maintained by diluting with fresh medium to a target cell density (C_{TAR}) of 1.5 $g \cdot L^{-1}$ every 48 hours.

2.2. Growth

Growth of batch cultures was measured by optical density that was calibrated against the dry weight. Absorbance in a 1.0 cm path length cell was recorded at 540 nm every two days and the dry weight was measured at 0, 10 and 20 days. The dry weight was measured by low-pressure vacuum filtration of a known volume of culture fluid through weighed 1.0 µm pore size 47 mm glass fiber filters (VWR, Norway) that were dried at 95°C for 48 hours. The productivity of semi-continuous cultures was measured by the dry weight and volume of broth removed. The concentration of nitrate in the broth was

measured with standard colorimetric reagents adapted to a 96-well microplate (Ringuet et al., 2011) using NADH:nitrate reductase (NECi Superior Enzymes, USA). The absorbance was measured at 540 nm (FLUOstar Optima, BMG Labtech, USA). Seven-point linear calibrations were included in each plate with r^2 values >0.996.

2.3. Lipid analysis

Lipids were extracted from lyophilized microalgae (~6 mg of sample) weighed using a precision balance (MX5, Mettler-Toledo). Lipid extraction was performed using 4.0 mL of chloroform:methanol solution (2:2.5 v/v) spiked with internal standard (Tripentadecanoin, C15:0 Triacylglycerol, Sigma-Aldrich). A bead mill (MagNA lyser, Roche, 0.1 mm glass beads) and a sonication bath were used for complete cell disruption. Total lipids were then recovered by addition of 2.5 mL aqueous Tris buffer (6 $g \cdot L^{-1}$ Tris, 58 $g \cdot L^{-1}$ NaCl, pH 7.5) followed by vortexing (10 seconds) and centrifugation (1500 rcf). The chloroform phase was removed and dried under a stream of nitrogen. Total crude lipid extracts were measured gravimetrically, and the fatty acid composition of neutral and polar lipids was measured by gas chromatography (GC). Separation of neutral and polar lipids was achieved by solid-phase extraction. Total lipid extracts were redissolved in 0.5 mL hexane:diethylether (7:1 v/v) and loaded onto 6 mL (1g) silica cartridges (Supelco®). Neutral lipids were first eluted with 10 mL of hexane:diethyl ether (7:1 v/v), then 10.0 mL of methanol:acetone:hexane (2:2:1 v/v/v) was added to elute the polar lipids. Each lipid fraction was then dried under a stream of nitrogen and the fatty acyl chains were derivatized to fatty acid methyl-esters (FAMEs) using acidic methanol (3.0 mL 5% H_2SO_4 in methanol, 70°C for 3h). The FAMEs were recovered by mixing (30 min) with 3.0 mL of hexane and quantitated by a GC fitted with a Flame Ionisation Detector (SCION 436, Bruker). The GC was operated without

injector sample split and was fitted with an Agilent CP-Wax 52 CB column. Supelco® 37-component standards were used for identification and quantitation of common fatty acids and additional standards were sourced for unusual unsaturated fatty acids (Larodan Fine Chemicals, Sweden). Each fatty acid was quantitated by linear regression of five-point calibrations (r^2 • .999) and blanks were included in the extraction procedure so that trace peaks derived from sample preparation could be eliminated. Internal standard recovery, accounting for sample losses and transesterification efficiency, averaged 95%.

2.4. Statistical methods

Batch cultures followed typical sigmoid growth patterns that comprised lag, exponential and stationary phases. The data was modeled and the differences amongst strains were evaluated using a nonlinear four-parameter logistic mixed-effects model using the R package *nlme* (Pinheiro & Bates 2006). The mixed-effects model contained both fixed (species) and random (bioreactor unit level) effects. The type of nonlinear mixed effects model used to describe the cell density (C_X, g·L^{-1}) over time was (eq. 1).

$$C_{X,ij} = \frac{\phi 2_i - \phi 1}{1 + \exp\left(\frac{\phi 3_i - t_{ij}}{\phi 4_i}\right)} + \varepsilon_{ij} \qquad (1)$$

In this expression $C_{X,ij}$ is the cell density (g·L^{-1}) in a bioreactor culture, i, at time t_{ij} (days); Parameter $\phi 1$ is the minimum dry weight (g·L^{-1}), the lower asymptote; $\phi 2$ is the maximum dry weight, the uppermost asymptote (g·L^{-1}); $\phi 3$ is the inflection point corresponding to the time of maximum growth (days) and $\phi 4$ is the slope parameter. A power variance model of the form $\mathrm{Var}(\varepsilon_{ij}) = \sigma^2|v_{ij}|^{2\delta}$ was used to significantly (LR = 118.7, $p < .001$) improve the analysis, where v_{ij} are variance covariates and δ corresponds to the variance parameters (Figs S1, S2). Random effects were included for

parameters $\phi 2$, $\phi 3$ and $\phi 4$; parameter $\phi 1$ was dropped from the random part of the model based on sequential model comparisons using Akaike's information criterion (AIC) statistics. Random effects were approximately normally distributed (Fig S3). After building the optimal model, the fixed-effect estimates of each parameter were obtained for each strain of algae and compared using the *t*-values and probabilities (Table S1c).

The productivity (P, $g \cdot L^{-1} \cdot d^{-1}$) was calculated using the logistic model fitted values of cell density (C_X) over time. The productivity in a photobioreactor at the j^{th} time was derived using a 1-hour time step ($t_j - t_{j-1} = 1$ hour, eq. 2) to generate high-resolution productivity curves, and the maximum value (P_{max}) was found.

$$P_j = \frac{C_{X,j} - C_{X,j-1}}{t_j - t_{j-1}} \qquad (2)$$

A curve was generated for each replicate culture and the mean and standard deviation of P_{max} for each variety ($n = 3$) was calculated. Next, the specific growth rate (k, d^{-1}) over time was calculated at high-resolution from P and C_x (Hulatt et al., 2017).

$$k_j = \frac{P_j}{C_{X,j}} \qquad (3)$$

The productivity (P, $g \cdot L^{-1} \cdot d^{-1}$) of semi-continuous cultivations maintained for 16-18 days was interpreted using a linear mixed-effects Analysis of Covariance (ANCOVA) model. The slopes and the intercepts were allowed to vary amongst the different strains, so that their respective intercepts are the average volumetric production at the start of semi-continuous cultivation ($g \cdot L^{-1} \cdot d^{-1}$) and their slopes describe the average change in productivity over time ($g \cdot L^{-1} \cdot d^{-2}$) for each species of microalga. The model included both random slopes and random intercepts for each experimental bioreactor unit.

2.5. Light

Light conversion efficiency was derived from P_{max} (batch cultures) and P_{10}, the productivity after 10 days of dilution (semi-continuous cultures). The photon flux incident on the photobioreactor, I ($mol \cdot L^{-1} \cdot d^{-1}$), was calculated (eq. 4).

$$I = \frac{f_{day}}{R_{PBR}} \qquad (4)$$

Where R_{PBR} is the photobioreactor illuminated surface area per unit culture volume ($m^2 \cdot L^{-1}$) and f_{day} is the average PAR photon flux (400-700 nm) over the surface of the photobioreactor ($mol \cdot m^{-2} \cdot d^{-1}$). The biomass yield on light was calculated (eq. 5).

$$Y_{X/mol} = \frac{P_{max}}{I} \qquad (5)$$

Where $Y_{X/mol}$ is the maximum biomass yield on light ($g \cdot mol^{-1}$). For semi-continuous cultures, P_{max} was substituted for P_{10}.

3. RESULTS & DISCUSSION

3.1. Batch cultures

In batch culture each of the five varieties reached maximum cell densities from 2.2 ± 0.9 to 3.4 ± 0.3 $g \cdot L^{-1}$ (Table 2). The growth patterns of four species were described using a logistic mixed-effects model (Fig 2), which provides a mechanistic interpretation of biomass accumulation. Despite strong growth *Macrochloris rubreoleum* formed cell aggregations, and so only the maximum cell density is presented for this variety. Table 2 also provides the model parameter estimates that characterize the average growth trajectory of each species of microalga. The model parameters, which describe important features of the growth curves, differed significantly between strains (F • 5.4, P • .002, Table 3) indicating that different species produced fundamentally different growth patterns. The maximum biomass ($\phi 2$) of

Chlamydomonas pulsatilla, for example, was significantly higher than each of the other two flagellate snow algae (all pairwise contrasts in Table S1c). The growth of *Raphidonema sempervirens* was characterized by a consistently extended lag phase, reaching maximum productivity after 14.3 ± 1.2 days (ϕ3). The productivity (P, $g \cdot L^{-1} \cdot d^{-1}$) and specific growth rate (k, d^{-1}) of each strain are presented in Fig 2. Maximum production (P_{max}) varied 2.5 fold between the different species, the highest productivity in batch culture attained by *C. pulsatilla* (0.58 ± 0.16 $g \cdot L^{-1} \cdot d^{-1}$) and the lowest productivity was obtained from *Chloromonas platystigma* (0.25 ± 0.09 $g \cdot L^{-1} \cdot d^{-1}$) (Table 5). On average, k_{max} ranged from 0.33 to 0.56 d^{-1} between species, equivalent to biomass doubling inside the photobioreactor every 1.8 to 3.0 days. Invariably, k_{max} occurred three to five days earlier than P_{max}.

3.2. Semi-continuous cultivation

To confirm that the high growth rates of batch cultures were repeatable and could be maintained in long-term cultures, the three most productive varieties (*C. pulsatilla*, *C. klinobasis* and *R. sempervirens*) were selected for cultivation in semi-continuous mode (Fig. 3). The productivity of semi-continuous cultures was modeled with a linear mixed effects ANCOVA (analysis of covariance) model that included separate slopes and intercepts (fixed effects) for each microalgae strain. In agreement with the batch cultures, significant differences in the intercepts ($F = 38.1$, $p < .001$, Table 4) confirmed that different varieties had fundamentally different growth rates. Again, *C. pulsatilla* consistently sustained the highest yields, measuring on average 0.57 $g \cdot L^{-1} \cdot d^{-1}$ at the start of the maintenance period (Table 4) and increasing on average to 0.63 $g \cdot L^{-1} \cdot d^{-1}$ after 10 days (Table 5). *Raphidonema sempervirens* initially produced the lowest yields in semi-continuous cultures (0.32 $g \cdot L^{-1} \cdot d^{-1}$, Table 4) and its productivity decreased to 0.21 $g \cdot L^{-}$

$^{1}\cdot d^{-1}$ after 10 days. On average, *C. pulsatilla* showed a weak increase in productivity over time (slope 0.006 $g\cdot L^{-1}\cdot d^{-2}$), whilst *R. sempervirens* showed a gradual reduction in productivity (slope 0.011 $g\cdot L^{-1}\cdot d^{-2}$) over the same period (Table 4). There were however no detectable differences in slope amongst the three species ($F = 2.2$, $p = .120$) and on average there was no overall change in productivity with time across all three varieties ($F = 0.6$, $p = .439$).

The results from batch cultures (section 3.1) and semi-continuous cultures are concordant. Together the data indicates that high productivity is possible from some cold-adapted strains at 6°C, but also shows that the species have substantially different maximum growth rates. In nature, different species and ecotypes adapt to their environment with strategies that are characterized by trade-offs between investments in resource acquisition/survival and growth rate (Litchman et al., 2015). Consequently this may translate to variation in maximum attainable yields in optimized cultures, and careful selection of individual strains is an essential step for achieving the maximum productivity.

Although research in the ecology of polar areas has indicated that microalgae can be productive in cold ecosystems, no previous studies have shown comparably high autotrophic productivity in low temperatures (i.e. sub-15°C). For example, a recent study reports productivity figures under 0.05 $g\cdot L^{-1}\cdot d^{-1}$ for ten strains native to Canada, cultivated at 10°C in autotrophic and mixotrophic conditions (Wang et al., 2016). Similarly, Abdelaziz et al. (2014) report in their screening study maximum productivity figures under 0.1 $g\cdot L^{-1}\cdot d^{-1}$ amongst Canadian strains cultivated at 10 and 22°C. The maximum productivity obtained in this study was over 6-fold higher in batch (0.58 $g\cdot L^{-1}\cdot d^{-1}$) and semi-continuous cultivations (0.63 $g\cdot L^{-1}\cdot d^{-1}$) at lower 6°C water temperature. This difference can be explained by a number of factors, especially strain selection and

photobioreactor design. The five species tested here, rather than being simply cold-tolerant, display the traits of true cryophiles; the three flagellate species (*C. pulsatilla*, *C klinobasis*, *C. platystigma*) for example remained highly motile (phototactic) close to freezing, becoming inactive at room temperature (Cavicchioli et al., 2011; Morgan-Kiss et al., 2006). The adaptation of microalgae to low water temperatures (e.g. genetic, epigenetic and short-term acclimation mechanisms) could provide solutions to increase productivity in industrial cultivation systems. A second variable is the supply of inorganic carbon for photosynthesis. At low water temperatures the solubility of CO_2 is increased, but the gas-liquid mass transfer of CO_2 is lower. Addition of concentrated CO_2 is essential for allowing maximum rates of carbon fixation, but does not seem to have been utilized in previous studies at low temperature.

3.3. Photosynthetic efficiency

To measure the photosynthetic efficiency of the photobioreactors, the biomass yield per mole photons PAR ($Y_{X/mol}$, $g \cdot mol^{-1}$) was calculated. In batch cultures the fastest growing strain, *C. pulsatilla*, recorded a PAR conversion efficiency of 1.23 ± 0.33 $g \cdot mol^{-1}$, reduced to 0.79 ± 0.03 $g \cdot mol^{-1}$ in semi-continuous cultures (Table 5). Although *R. sempervirens* performed strongly in batch culture, peaking at 0.91 ± 0.10 $g \cdot mol^{-1}$, in semi-continuous mode, it ultimately recorded the lowest PAR conversion efficiency at 0.23 ± 0.12 $g \cdot mol^{-1}$. The values for *C. pulsatilla* are comparable to those predicted by de Mooij et al. (2014) and the upper values discussed by Vejrazka et al. (2012) for related *Chlamydomonas reinhardtii* under similar incident irradiance conditions. These figures correspond to approximately 12% and 8% PAR energy conversion efficiency, which is equivalent to ~5% and ~3% total solar energy conversion (see supporting text). Such high light conversion rates are unlikely to be obtained in stronger light, because the

quantum yield invariably decreases with increasing irradiance and the influence of temperature on photosynthetic rate is greater. Nevertheless, the data supports the other results, demonstrating that low-temperature cultivation systems can still offer high light utilization efficiency. The light environment experienced by an algal cell is a function of the incident irradiance, the cell density and the mixing characteristics (i.e. the transition of a cell along the internal light gradient) of the photobioreactor (Béchet et al., 2013). The effect of strong light should be investigated further to determine the efficiency at the higher light intensities that might be experienced by cells in outdoor cultivation systems, although various photon management strategies can be used to mitigate the effects of high irradiance (Ooms et al., 2016). At cooler, higher latitudes, annual changes in irradiance and photoperiod are much larger than in equatorial regions. Therefore, microalgae cultivated outdoors must be able to cope with both high and low light conditions. The terrestrial strains tested in this work are potentially well suited to such variable light regimes. For example, *Raphidonema* may utilize a large pool of xanthophyll cycle pigments for non-photochemical quenching in high light conditions (Leya et al., 2009) and closely-related *Koliella* is also able to survive the prolonged seasonal periods of darkness in polar regions (Baldisserotto et al., 2005). Many microalgae are also able to utilize exogenous organic carbon sources, and so photoheterotrophic cultivation might provide an opportunity to improve microalgae productivity in low light and temperature conditions (Wang et al., 2016).

3.3. Lipids and fatty acids in batch cultures

In batch cultures, each of the five species accumulated total crude lipid between 10 and 20 days, reaching up to 39% of the dry cell mass (Table 2). The accumulation of lipid

was comparable amongst the different varieties, with an average increase of +16% total lipid from day 10 to day 20 (Fig S4). Snow algae lipids were fractionated into neutral lipids (predominantly triglycerides; TAG) and polar lipids (membrane lipids), and the constituent fatty acids were analyzed. Fatty acids in polar lipids decreased from day 10 to day 20, whilst those in neutral lipids systematically increased in abundance (Fig 4).

The three flagellate snow algae largely accumulated polyunsaturated fatty acids (PUFAs) in neutral lipids. Each *Chlamydomonas* strain accumulated C16:3, C16:4, C18:1, C18:2 and C18:3*n*-3, whilst the neutral lipids of *Chloromonas* were also characterized by a large increase in C18:3*n*-3 from 10 to 20 days (Fig 4). *Macrochloris rubreoleum* and *R. sempervirens* behaved differently, each generally accumulating only C18 series fatty acids, especially monounsaturated fatty acids (MUFAs). *Macrochloris rubreoleum* accumulated both C18:1*n*-9 and C18:1*n*-7 isomers, C18:2*n*-6, and smaller amounts of C18:3*n*-3, whilst neutral lipid production by *R. sempervirens* was comprised almost entirely by just one type of monounsaturated fatty acid, C18:1*n*-9 (oleic acid).

The fatty acids 16:0 and 18:3*n*-3 were abundant in the polar lipids of each of the five species (Fig 5). The flagellate strains *Chlamydomonas* sp. and *C. platystigma* were also characterized by polar lipids containing large amounts of C16:3 and C16:4 acyl chains, whilst *M. rubreoleum* contained C18 series MUFA and PUFA fatty acids. *Raphidonema sempervirens* was the only strain to produce long chain PUFAs, yielding C20:5*n*-3 (eicosapentanoic acid, EPA) at a maximum 6.6 wt% of the total FAMEs at day 10.

For fuels, TAG is the most valuable lipid feedstock because it is a convenient precursor molecule for upgrading to biodiesel (Hu et al., 2008; Olmstead et al., 2013). A single microalga can contain dozens of different TAG molecules with fatty acyl chains in various *sn*-positions (Řezanka et al., 2014) and the profiles in Fig 4 are the average

patterns for each species. The model oleaginous microalga *Nannochloropsis* primarily accumulates saturated and monounsaturated fatty acids C16:0 (42%), C16:1*n*-7 (29%) and represents a standard for comparative purposes (Fig S5). Each of the Arctic varieties however primarily accumulated mono and polyunsaturated fatty acids in neutral lipids, which is consistent with observations of PUFA-rich TAG in other snow algae (Řezanka et al., 2014), and may be an important feature of lipid products from similar cold-adapted strains. Whilst high PUFA content is desirable for food and feeds, it also impacts the suitability for biodiesel, by modifying the oxidative stability and cold-flow properties of its fuel derivatives (Olmstead et al., 2013). Hydrotreatment however, may offer an alternative method for upgrading microalgal oils to renewable (green) diesel fuel (Elliott et al., 2013).

3.4. Comparison of low temperature productivity with other studies

The performance of microalgae is often difficult to compare between studies due to differences in cultivation conditions and the variables that limit growth rate. For example, the interacting effects of irradiance, optical path length, temperature, nutrient supply, CO_2 supply and cell density each affect productivity. Therefore, to put the data in context, the results from this study were compared with similar designs of photobioreactors operated at warmer temperatures (Fig 6a) and with data from an exhaustive meta-analysis that has compiled data from 60 years of intensive photobioreactor cultivation experiments (Fig 6b) (Granata 2017). In each of the comparisons, the productivity of the low temperature systems remained in the center of the defined ranges, i.e. broadly comparable to many other warm-water studies. These results show that, although low temperature invariably reduces maximum metabolic rate

(Ahlgren et al., 1987; Falkowski & Raven 2013; Raven & Geider 1988), the reductions in yield at low temperatures may not be as great as expected.

4. CONCLUSIONS

At a temperature of 6°C, maximum productivity reached 0.63 $g \cdot L^{-1} \cdot d^{-1}$ and lipid content up to 39% was attained with the snow alga *Chlamydomonas pulsatilla*. The neutral lipids of each species were comprised by a large proportion of mono and polyunsaturated fatty acids, which may find applications in industrial production. Overall, the results indicate that selection of alternative varieties of microalgae from polar environments may provide an opportunity to, at least partially, mitigate the reduced yields associated with lower water temperatures, or avoid the need to invest large amounts of heat energy in large-scale microalgae cultivation systems.

SUPPORTING INFORMATION

Additional data supporting this study are available with the online version of this article.

CONTRIBUTIONS

CJH and OB designed the study and collected the data. CJH, KV, RHW, ESE and OB wrote the manuscript.

COMPETING INTERESTS

The authors declare no competing interests.

ACKNOWLEDGEMENTS

The authors are grateful to Nordland County Govornment for funding this research as part of the project 'Bioteknologi– en framtidsrettet næring'. The authors are thankful for assistance from the technical staff and the facilities at the Nord University research station. Tim Granata (Lucerne University) kindly supplied the literature data from his meta-analysis (Fig. 6b) and Thomas Leya (CCCryo) is thanked for his expert advice on cryophilic microalgae.

REFERENCES

1. Abdelaziz, A.E., Leite, G.B., Belhaj, M.A., Hallenbeck, P.C., 2014. Screening microalgae native to Quebec for wastewater treatment and biodiesel production. Bioresour. Technol. 157, 140-148.
2. Ahlgren, G., 1987. Temperature functions in biology and their application to algal growth constants. Oikos 49, 177-190.
3. Baldisserotto, C., Ferroni, L., Andreoli, C., Fasulo, M. P., Bonora, A., Pancaldi, S., 2005. Dark-acclimation of the chloroplast in *Koliella antarctica* exposed to a simulated austral night condition. Arct. Antarct. Alp. Res. 37, 146-156.
4. Béchet, Q., Shilton, A., Park, J.B.K., Craggs, R.J., Guieysse, B., 2011. Universal temperature model for shallow algal ponds provides improved accuracy. Environ. Sci. Technol. 45, 3702-3709.
5. Béchet, Q., Shilton, A., Guieysse, B., 2013. Modeling the effects of light and temperature on algae growth: state of the art and critical assessment for productivity prediction during outdoor cultivation. Biotechnol. Adv. 31, 1648-1663.

6. Bernard, O., Rémond. B., 2012. Validation of a simple model accounting for light and temperature effect on microalgal growth. Bioresour. Technol. 123, 520-527.
7. Bischoff, H.W., Bold, H.C., 1963. Some soil algae from Enchanted Rock and related algal species. No. 4. University of Texas Publications.
8. Canadell, J.G., Schulze, E.D., 2014. Global potential of biospheric carbon management for climate mitigation. Nat. Commun. 5, doi: 10.1038/ncomms6282.
9. Cavicchioli, R., Charlton, T., Ertan, H., Omar, S. M., Siddiqui, K. S., Williams, T. J., 2011. Biotechnological uses of enzymes from psychrophiles. Microb. Biotechnol. 4, 449-460.
10. Chisti, Y., 2012. Raceways-based production of algal crude oil, in: Posten, C., Walter, C., (Eds.), Microalgal Biotechnology: Potential and Production. de Gruyter, Berlin, pp. 113-146.
11. Chisti, Y., 2013. Constraints to commercialization of algal fuels. J. Biotechnol. 167, 201-214.
12. de Mooij, T., Janssen, M., Cerezo-Chinarro, O., Mussgnug, J.H., Kruse, O., Ballottari, M., Bassi, R., Bujaldon, S., Wollman, F.A., Wijffels, R.H., 2015. Antenna size reduction as a strategy to increase biomass productivity: a great potential not yet realized. J. Appl. Phycol. 27, 1063-1077.
13. Elliott, D.C., Hart, T.R., Schmidt, A.J., Neuenschwander, G.G., Rotness, L.J., Olarte, M.V., Zacher, A.H., Albrecht, K.O., Hallen, R.T., Holladay, J.E., 2013. Process development for hydrothermal liquefaction of algae feedstocks in a continuous-flow reactor. Algal Res. 2, 445-454.

14. Endres, C.H., Roth, A., Brück, T.B., 2016. Thermal Reactor Model for Large-Scale Algae Cultivation in Vertical Flat Panel Photobioreactors. Environ. Sci. Technol. 50, 3920-3927.

15. Falkowski, P.G., Raven, J.A., 2013. Aquatic photosynthesis, Princeton University Press.

16. Georgianna, D.R., Mayfield, S.P., 2012. Exploiting diversity and synthetic biology for the production of algal biofuels. Nature 488, 329-335.

17. Gounot, A.M., Russell, N.J., 1999. Physiology of cold-adapted microorganisms, in: Margesin, R., Schinner, F. (Eds), Cold-adapted Organisms. Springer, Berlin, pp. 33-55.

18. Granata, T., 2017. Dependency of Microalgal Production on Biomass and the Relationship to Yield and Bioreactor Scale-up for Biofuels: a Statistical Analysis of 60+ Years of Algal Bioreactor Data. Bioenergy Res. 10, 267-287.

19. Guccione, A., Biondi, N., Sampietro, G., Rodolfi, L., Bassi, N., Tredici, M.R., 2014. *Chlorella* for protein and biofuels: from strain selection to outdoor cultivation in a Green Wall Panel photobioreactor. Biotechnol. Biofuels 7, doi: 10.1186/1754-6834-7-84.

20. Hori, K., Maruyama, F., Fujisawa, T., Togashi, T., Yamamoto, N., Seo, M., Sato, S., Yamada, T., Mori, H., Tajima, N., Moriyama, T., 2014. *Klebsormidium flaccidum* genome reveals primary factors for plant terrestrial adaptation. Nat. Commun. 5, doi:10.1038/ncomms4978.

21. Hu, Q., Sommerfeld, M., Jarvis, E., Ghirardi, M., Posewitz, M., Seibert, M., Darzins, A., 2008. Microalgal triacylglycerols as feedstocks for biofuel production: perspectives and advances. Plant J. 54, 621-639.

22. Hulatt, C.J., Thomas, D.N., 2011. Productivity, carbon dioxide uptake and net energy return of microalgal bubble column photobioreactors. Bioresour. Technol. 102, 5775-5787.

23. Hulatt, C.J., Wijffels, R.H., Bolla, S., Kiron, V., 2017. Production of Fatty Acids and Protein by *Nannochloropsis* in Flat-Plate Photobioreactors. PLoS ONE, 12, doi:10.1371/journal.pone.0170440.

24. Komárek. J., Nedbalová, L., 2007. Green Cryosestic Algae, in: Sekbach, J. (Ed.), Algae and Cyanobacteria in Extreme Environments. Springer, Netherlands, pp. 321-342.

25. Leya, T., Rahn, A., Lütz, C., Remias, D., 2009. Response of arctic snow and permafrost algae to high light and nitrogen stress by changes in pigment composition and applied aspects for biotechnology. FEMS Microbiol. Ecol. 67, 432-443.

26. Litchman, E., Edwards, K.F., Klausmeier, C.A., 2015. Microbial resource utilization traits and trade-offs: implications for community structure, functioning, and biogeochemical impacts at present and in the future. Front. Microbiol. 6, doi: 10.3389/fmicb.2015.00254.

27. Lutz, S., Anesio, A.M., Raiswell, R., Edwards, A., Newton, R.J., Gill, F., Benning, L.G., 2016. The biogeography of red snow microbiomes and their role in melting arctic glaciers. Nat. Commun. 7, doi: 10.1038/ncomms11968.

28. Lyon, B.R., Mock, T. 2014. Polar microalgae: new approaches towards understanding adaptations to an extreme and changing environment. Biology 3, 56-80.

29. Matassa, S., Boon, N., Pikaar, I., Verstraete, W., 2016. Microbial protein: future sustainable food supply route with low environmental footprint. Microb. Biotechnol. 9, 568-575.

30. Mock, T., Otillar, R.P., Strauss, J., McMullan, M., Paajanen, P., Schmutz, J., Salamov, A., Sanges, R., Toseland, A., Ward, B.J., Allen, A.E., Dupont, C.L., Frickenhaus, S., Maumus, F., Veluchamy, A., Wu, T., Barry, K.W., Falciatore, A., Ferrante, M.I., Fortunato, A.E., Glöckner, G., Gruber, A., Hipkin, R., Janech, M.G., Kroth, P.G., Leese, F., Lindquist, E.A., Lyon, B.R., Martin, J., Mayer, C., Parker, M., Quesneville, H., Raymond, J.A., Uhlig, C., Valas, R.E., Valentin, K.U., Worden, A.Z., Armbrust, E.V., Clark, M.D., Bowler, C., Green, B.R., Moulton, V., van Oosterhout, C., Grigoriev, I.V., 2017. Evolutionary genomics of the cold-adapted diatom *Fragilariopsis cylindrus*. Nature 541, 536-540.

31. Moody, J.W., McGinty, C.M., Quinn, J.C., 2014. Global evaluation of biofuel potential from microalgae. P. Natl. Acad. Sci. USA 111, 8691-8696.

32. Morgan-Kiss, R.M., Priscu, J.C., Pocock, T., Gudynaite-Savitch, L., Huner, N.P.A., 2006. Adaptation and acclimation of photosynthetic microorganisms to permanently cold environments. Microbiol. Mol. Biol. Rev. 70, 222-252.

33. Olmstead, I.L.D., Hill, D.R.A., Dias, D.A., Jayasinghe, N.S., Callahan, D.L., Kentish, S.E., Scales, P.J., Martin, G.J.O., 2013. A quantitative analysis of microalgal lipids for optimization of biodiesel and omega-3 production. Biotechnol. Bioeng. 110, 2096-2104.

34. Ooms, M.D., Dinh, C.T., Sargent, E.H., Sinton, D., 2016. Photon management for augmented photosynthesis. Nat. Commun. 7, doi:10.1038/ncomms12699.

35. Pinheiro, J., Bates, D.M., 2006. Mixed-effects models in S and S-PLUS. Springer, New York.

36. Raven, J.A., Geider, R.J., 1988. Temperature and algal growth. New Phytol. 110, 441-461.

37. Řezanka, T., Nedbalová, L., Procházková, L., Sigler, K. 2014. Lipidomic profiling of snow algae by ESI-MS and silver-LC/APCI-MS. Phytochemistry 100, 34-42.

38. Ringuet, S., Sassano, L., Johnson, Z.I., 2011. A suite of microplate reader-based colorimetric methods to quantify ammonium, nitrate, orthophosphate and silicate concentrations for aquatic nutrient monitoring. J. Environ. Monit. 13, 370-376.

39. Rodolfi, L., Zittelli, G.C., Bassi, N., Padovani, G., Biondi, N., Bonini, G., Tredici, M. R., 2009. Microalgae for oil: Strain selection, induction of lipid synthesis and outdoor mass cultivation in a low-cost photobioreactor. Biotechnol. Bioeng. 102, 100-112.

40. Thomas, D.N., Dieckmann, G.S., 2002. Antarctic sea ice--a habitat for extremophiles. Science 295, 641-644.

41. Varshney, P., Mikulic, P., Vonshak, A., Beardall, J., Wangikar, P.P., 2015. Extremophilic micro-algae and their potential contribution in biotechnology. Bioresour. Technol. 184, 363-372.

42. Vejrazka, C., Janssen, M., Streefland, M., Wijffels, R.H., 2012. Photosynthetic efficiency of Chlamydomonas reinhardtii in attenuated, flashing light. Biotechnol. Bioeng. 109, 2567-2574.

43. Wang, Y-Z., Hallenbeck, P.C., Leite, G.B., Paranjape, K., Huo, D-Q., 2016. Growth and lipid accumulation of indigenous algal strains under photoautotrophic and mixotrophic modes at low temperature. Algal. Res. 16, 195-200.

FIGURE CAPTIONS

Figure 1. Diagram of the experimental photobioreactors with dimensions and culture volume.

Figure 2. Growth patterns in batch culture. (a) Uppermost panels show the accumulation of biomass (C_X) by four species of microalgae. Grey lines demarcate the predicted values of individual logistic models fitted to replicate cultures. Red lines are predicted values for each species from the mixed model. (b) Lowermost panels show the volumetric production (P, solid lines) and the specific growth rate (*k*, dashed lines).

Figure 3. Productivity in semi-continuous cultures. (a) Left-hand panels show the changes in biomass (C_X) before and during semi-continuous cultivation of the three most productive species. (b) Right-hand panels show the productivity (P) over time. The fitted lines are the fixed-effects (average for each species) from the linear mixed-effects (ANCOVA) model.

Figure 4. Patterns of neutral lipid accumulation. Left-hand columns show the proportion of total fatty acids comprised by neutral lipids (uppermost colored segments) after 10 and 20 days cultivation. Right-hand panels show the patterns of fatty acid accumulation

in the neutral lipids. Grey and white bars indicate 10 and 20 day cultivation times respectively.

Figure 5. Fatty acids in polar lipids. Changes in fatty acids (as methyl esters, $mg.g^{-1}$ dry weight) in the polar lipids of five species. Grey and white bars indicate 10 and 20 day cultivation times respectively.

Figure 6. Comparison of productivity at low temperature with other studies (a) Non-exhaustive comparison of snow algae photobioreactor productivity at 6°C with similar photobioreactor designs (comparable irradiance, light path length and CO_2 supply) at 25 and 26°C (Guccione et al., 2014; Hulatt & Thomas 2011; Rodolfi et al., 2009). (b) Exhaustive comparison of snow algae photobioreactor productivity at 6°C with 60-years of intensive photobioreactor cultivation (Granata 2017). Colored points are the mean for each species in batch and semi-continuous cultures and a horizontal jitter is applied for visualization, x-axis unitless.

TABLES

Table 1. Strain information. Species identities (strain ID) are from the CCCryo database (see methods) with the habitat and latitude from which strains were originally collected.

Name	Class	strain ID	Habitat	Motility	Lat.	Long.
Chlamydomonas klinobasis	Chlorophyceae	194-04	snow field	biflagellate	78°55N	11°53E
Chlamydomonas pulsatilla	Chlorophyceae	050-99	snow field	biflagellate	79°39N	11°00E
Chloromonas platystigma	Chlorophyceae	002b-99	snow field	biflagellate	78°58N	11°36E
Raphidonema sempervirens	Trebouxiophyceae	011a-99	snow field	no	78°58N	11°36E
Macrochloris rubreoleum	Chlorophyceae	020-99	hard substrate	[+]zoospores	79°16N	11°46E

[+]*M. rubreoluem* produces biflagellate zoospores during its life cycle but is otherwise non-motile.

Table 2. Batch growth statistics. The maximum dry weight ($g \cdot L^{-1}$) and maximum crude lipid (% dry weight) are recorded after 20 days of batch cultivation. Maximum inorganic Nitrogen (nitrate) uptake is the difference between two measurements over 48 hours. The fixed effects parameters from the logistic mixed-effects model are provided.

Strain	Batch growth statistics			Logistic mixed-model fixed effects parameters*			
	Max dwt ($g \cdot L^{-1}$)	Max Lipid (%)	Max N uptake ($mM\ NO_3^- \cdot L^{-1} \cdot d^{-1}$)	$\phi 1$ ($g \cdot L^{-1}$)	$\phi 2$ ($g \cdot L^{-1}$)	$\phi 3$ (days)	$\phi 4$ (scale)
Chlamydomonas klinobasis	2.59 (0.46)	34.4 (4.4)	1.28 (1.34)	0.08 (0.02)	2.52 (0.19)	8.68 (0.84)	1.87 (0.19)
Chlamydomonas pulsatilla	3.37 (0.26)	39.2 (7.3)	1.59 (0.15)	0.09 (0.02)	3.26 (0.27)	7.10 (1.18)	1.30 (0.25)
Chloromonas platystigma	2.16 (0.89)	31.4 (8.2)	1.07 (1.07)	-0.07 (0.02)	2.17 (0.27)	10.30 (1.20)	2.21 (0.26)
Raphidonema sempervirens	2.67 (0.16)	28.2 (2.2)	0.77 (0.60)	0.07 (0.02)	2.91 (0.29)	14.26 (1.21)	1.95 (0.26)
Macrochloris rubreoleum	2.06 (0.85)	37.5 (2.1)	0.95 (0.42)	—	—	—	—

[+]The model parameters are: $\phi 1$, lower asymptote; $\phi 2$, upper asymptote; $\phi 3$, time of maximum growth; $\phi 4$, scale parameter. See methods and supporting information for further details.

Table 3. Results of logistic nonlinear mixed effects model of batch cultivation kinetics. Tests for the effect of *Strain* (between-species differences) are presented for each of the four parameters.

Parameter		num *df*	den *df*	*F*	p
$\phi 1$	intercept	1	105	885.0	< .001
	Strain	3	105	153.7	< .001***
$\phi 2$	intercept	1	105	1860.1	< .001
	Strain	3	105	6.8	< .001***
$\phi 3$	intercept	1	105	172.2	< .001
	Strain	3	105	16.6	< .001***
$\phi 4$	intercept	1	105	417.9	< .001
	Strain	3	105	5.4	.002**

[+]Significant differences at the 99% (**) and 99.9% level (***) are indicated.
[++]Parameter pairwise contrasts between strains are available in Table S1c.

Table 4. Results of Analysis of Covariance (ANCOVA) linear mixed-effects model of biomass production in semi-continuous cultivations. (a) Fixed effect parameter estimates (*M* ± *SE*) for each strain including the intercepts ($g \cdot L^{-1} \cdot d^{-1}$ dry weight at day zero) and slopes ($g \cdot L^{-1} \cdot d^{-2}$). (b) Analysis of variance table presenting the main effects and interaction (i.e. different slopes between species).

(a)

Strain	intercept	slope
Chlamydomonas klinobasis	0.39 (0.07)	-0.002 (0.007)
Chlamydomonas pulsatilla	0.57 (0.05)	0.006 (0.005)
Raphidonema sempervirens	0.32 (0.07)	-0.011 (0.007)

(b)

Factor	num *df*	den *df*	*F*	p
intercept	1	65	581.2	< .001
day	1	65	0.6	.439
strain	2	7	38.1	< .001***
day × strain	2	65	2.2	.120

Table 5. Growth rate and photosynthetic efficiency. Summary statistics for batch and semi-continuous cultures. Values are the maximum growth rate in batch or semi-continuous cultures (P_{max} or P_{10}) and the light energy conversion efficiency expressed as grams of biomass produced per mol of PAR photons, *M* (± *SD*).

	Batch cultures			Semi-continuous		
Species	P_{max} ($g \cdot L^{-1} \cdot d^{-1}$)	$g \cdot mol^{-1}$	*n*	P_{10} ($g \cdot L^{-1} \cdot d^{-1}$)	$g \cdot mol^{-1}$	*n*
Chlamydomonas klinobasis	0.33 (0.08)	0.71 (0.16)	3	0.36 (0.10)	0.45 (0.12)	3
Chlamydomonas pulsatilla	0.58 (0.16)	1.23 (0.33)	3	0.63 (0.03)	0.79 (0.03)	4
Chloromonas platystigma	0.25 (0.09)	0.53 (0.20)	3	—	—	—
Raphidonema sempervirens	0.43 (0.04)	0.91 (0.10)	3	0.18 (0.10)	0.23 (0.12)	3

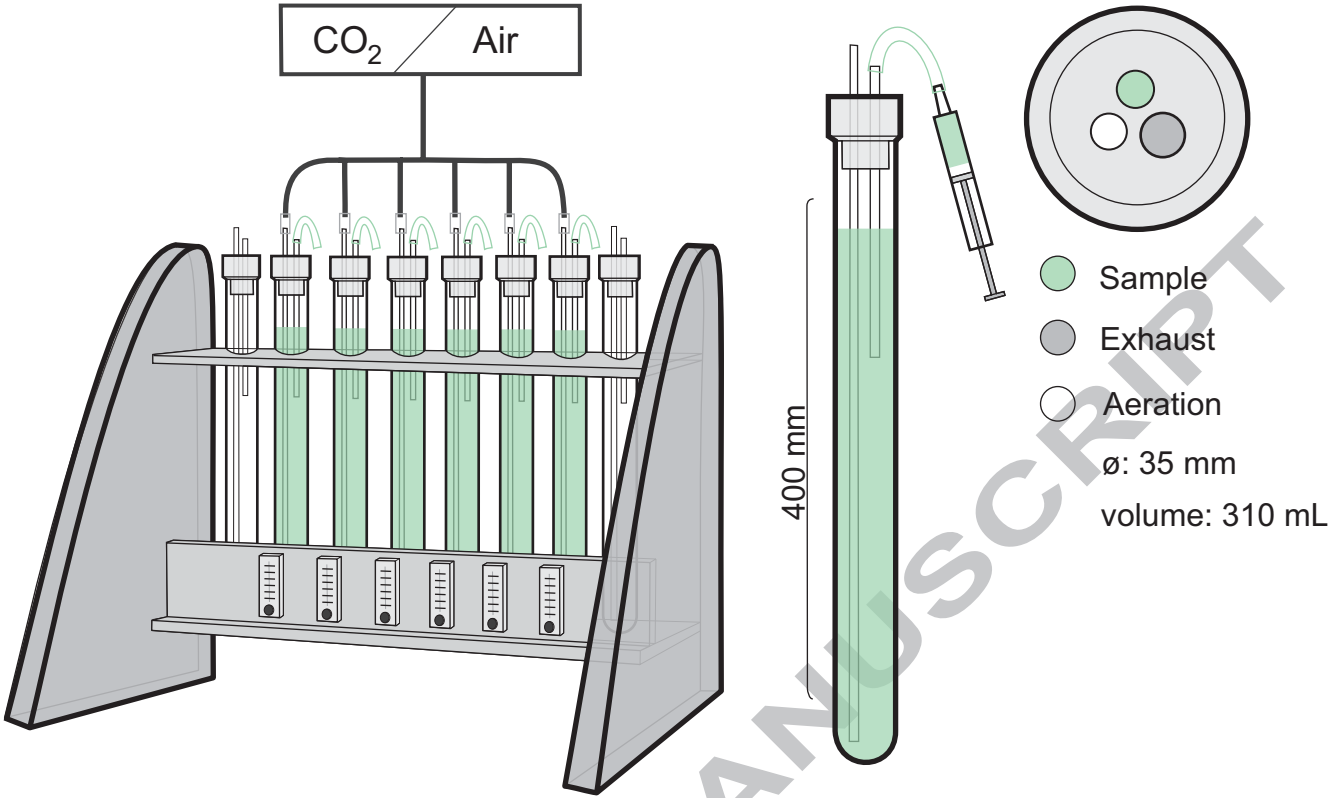

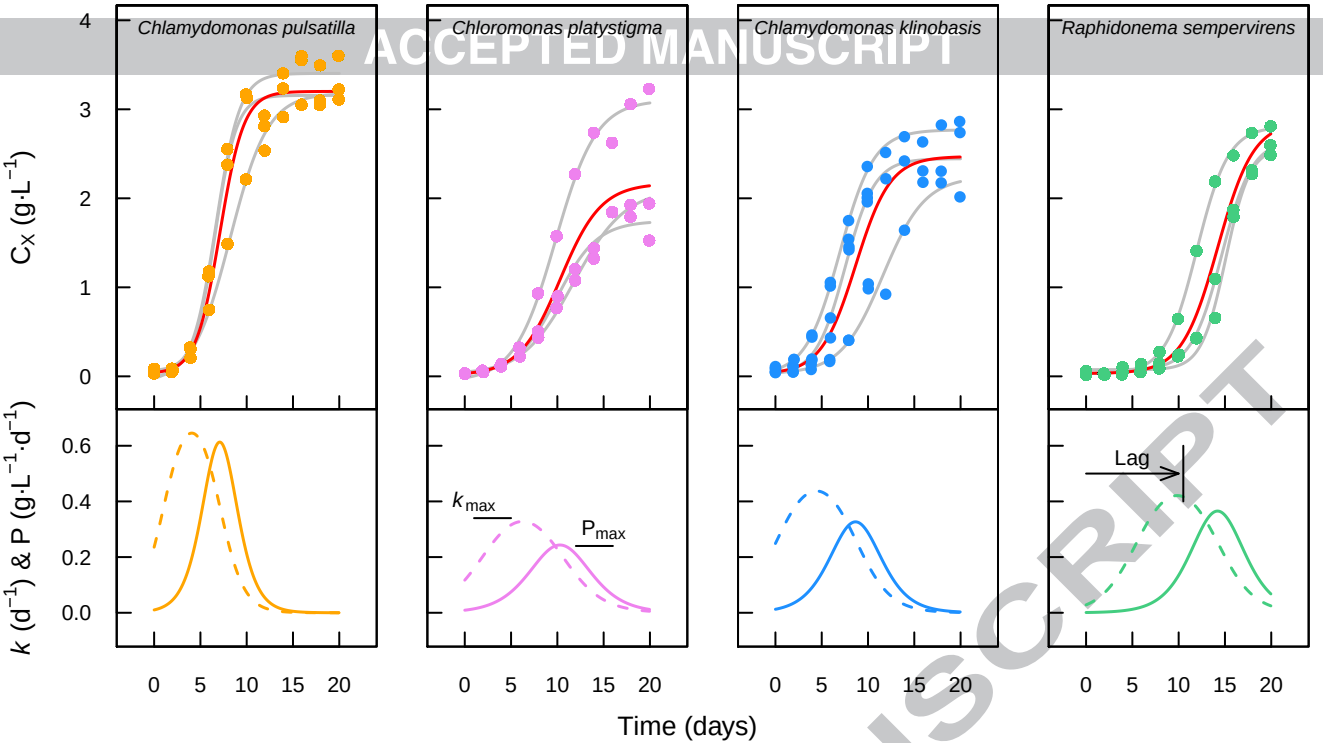

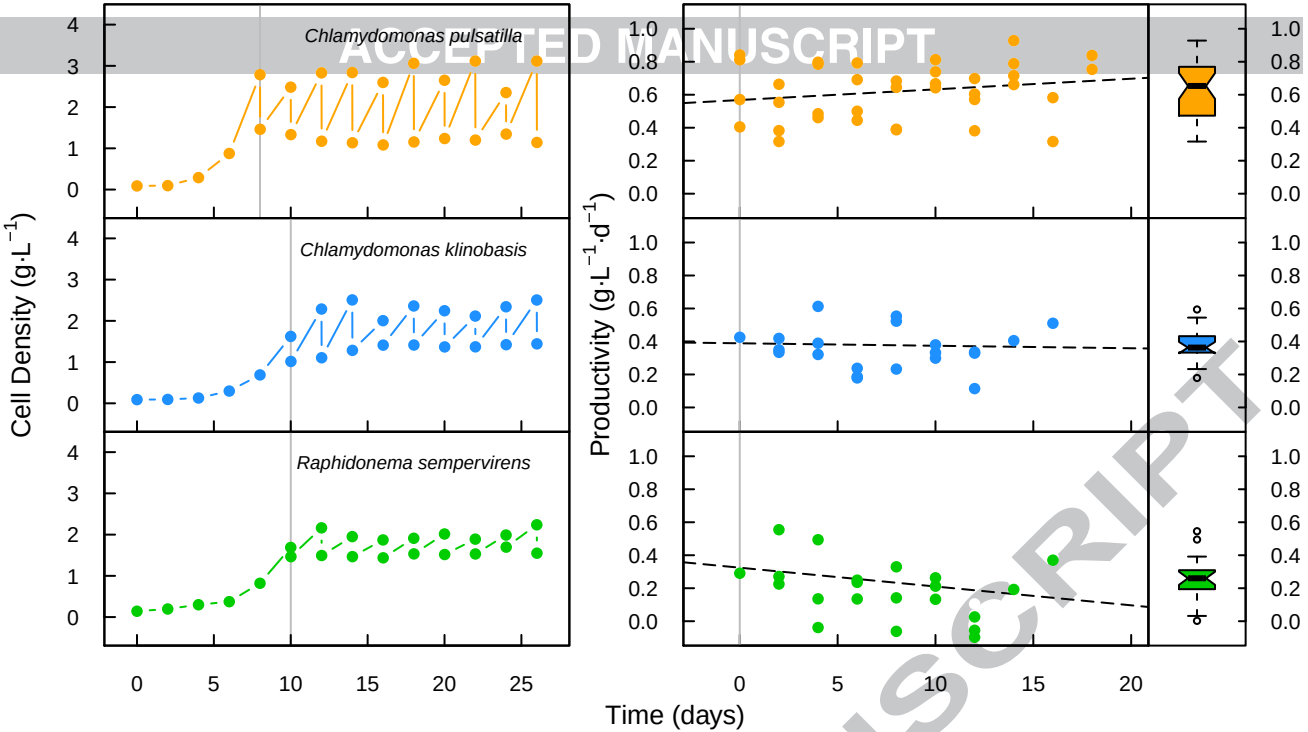

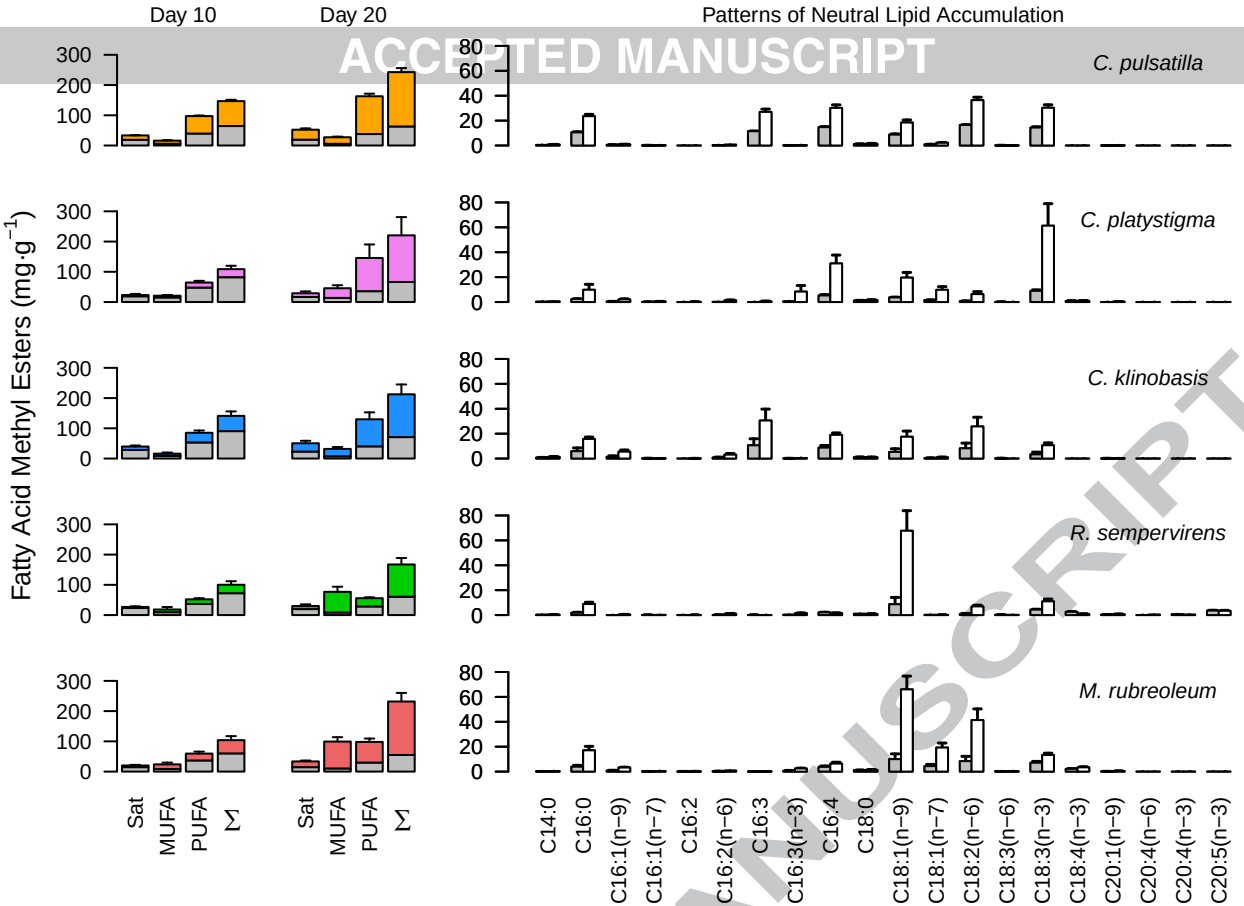

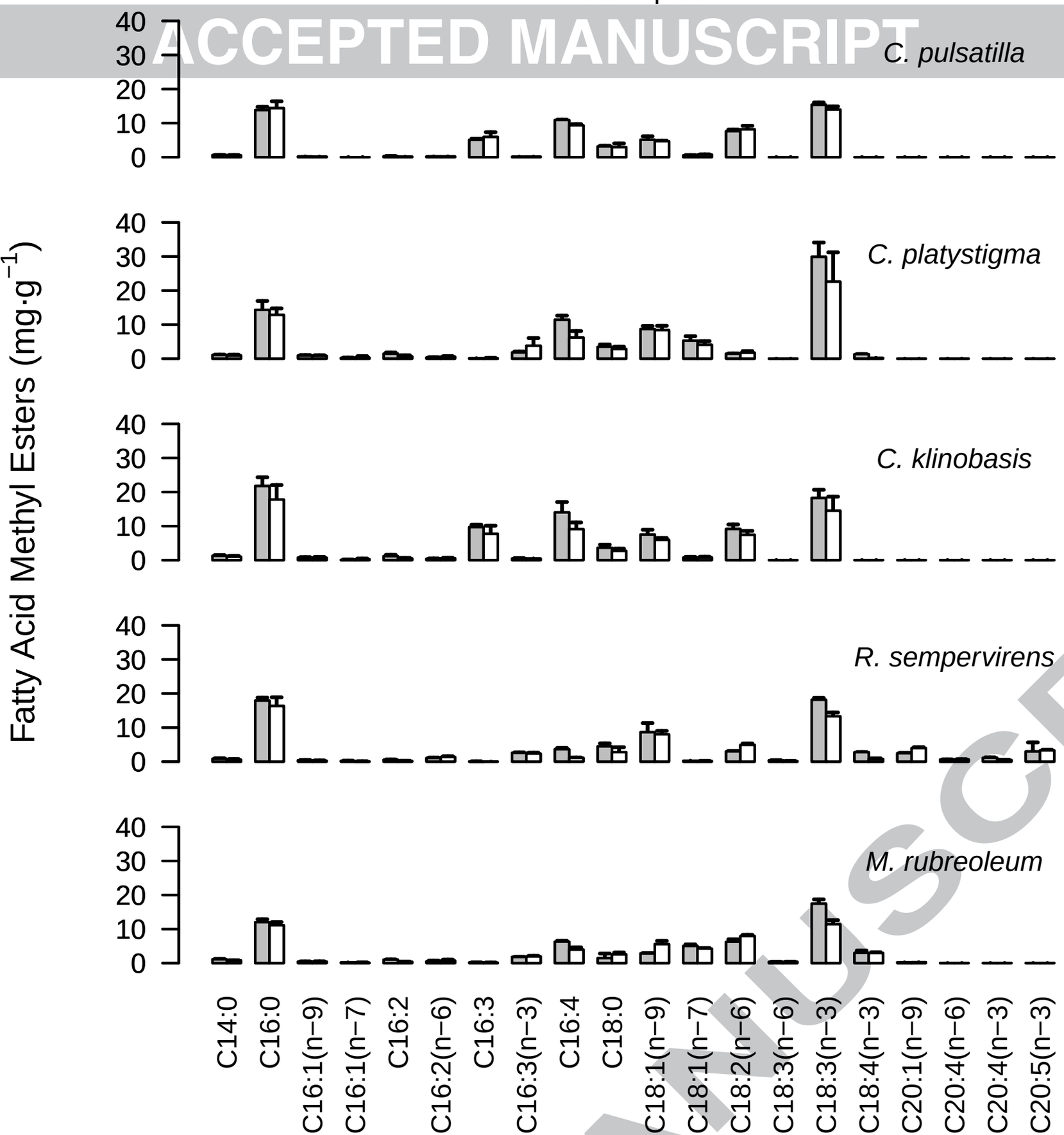

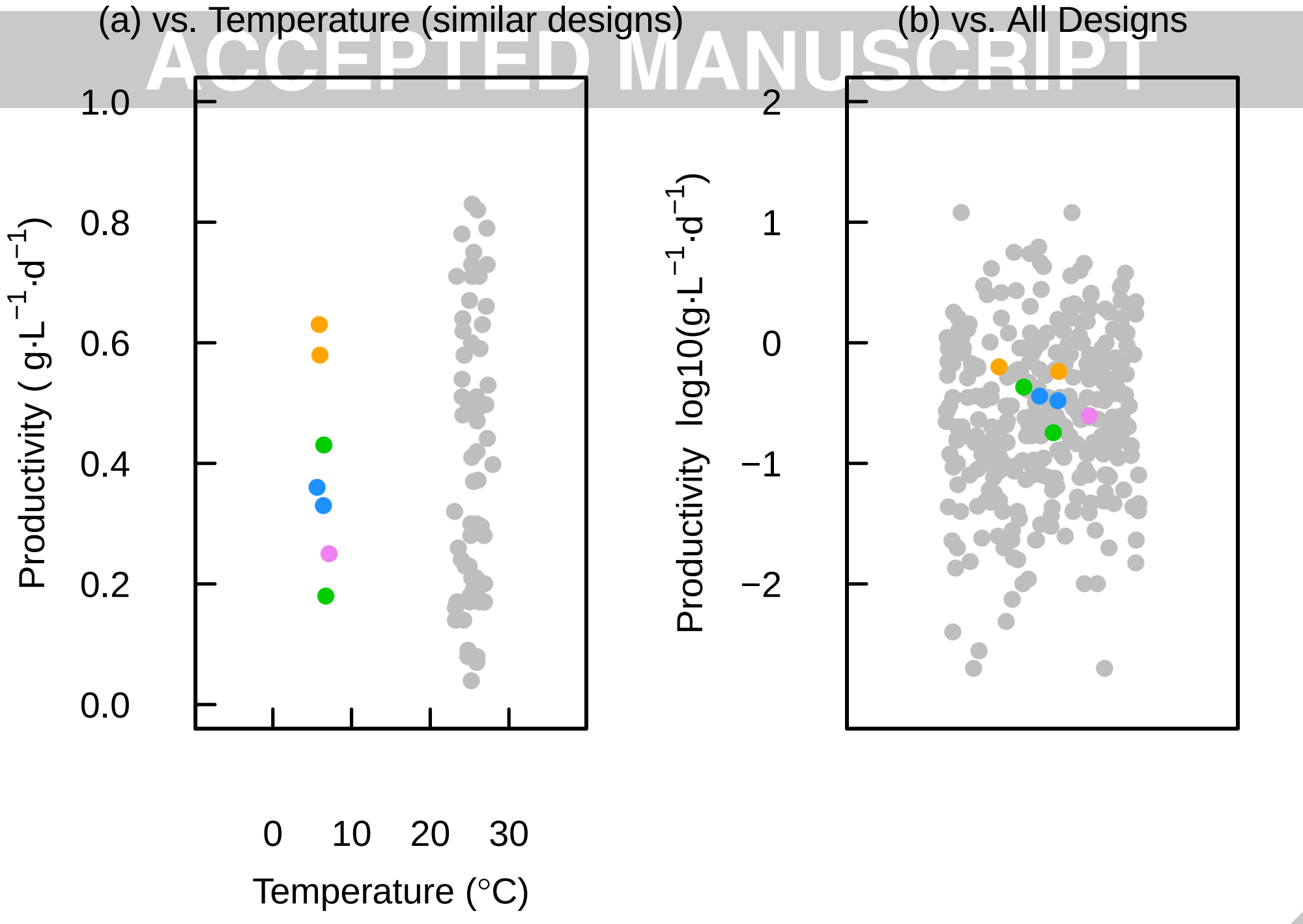

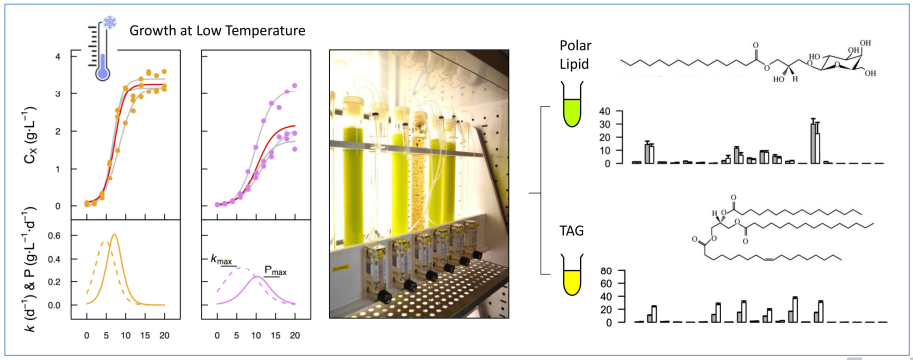

HIGHLIGHTS

1. Polar snow algae cultivated in low temperature photobioreactors.
2. Productivities up to 0.63 $g \cdot L^{-1} \cdot d^{-1}$ (dry weight) were attained.
3. Neutral lipids (TAG) were comprised by large amounts of MUFAs/PUFAs.
4. Cold adapted microalgae may offer improved performance in lower temperatures.